Molecular solvent model for an electrical double layer: Reference hypernetted chain results for potassium chloride solutions

G. M. Torrie
Department of Mathematics and Computer Science, Royal Military College, Kingston, Ontario K7K 5L0, Canada

P. G. Kusalik[a] and G. N. Patey
Department of Chemistry, University of British Columbia, Vancouver, B. C. V6T 1Y6, Canada

(Received 27 September 1988; accepted 22 November 1988)

The reference hypernetted-chain theory is solved for the structure of the double layer at the surface of large spherical macroions in a wholly molecular model of aqueous KCl. Detailed results are reported for the solvent and ionic structure throughout the double layer for surface charges up to 0.175 C m^{-2} and salt concentrations of 0.1 to 1.0 M. Concentration effects on the short-range structural features of the interface are discussed and related to the behavior of the same model at infinite dilution. There is a very rapid neutralization of the surface charge by a Coulombic adsorption of counterions into a narrow region near contact beyond which the system responds as though to a much lower effective surface charge. The relationship of these results to the properties of continuum solvent models and the implications for the electrostatic potential and differential capacitance of the double layer are discussed.

I. INTRODUCTION

This paper is the third in a series describing results of the reference hypernetted-chain (RHNC) theory for Hamiltonian models of aqueous electrical double layers. Our principal objective in this work has been to obtain theoretical predictions for the detailed microscopic structure of the solution side of the electrified interface for a model in which the solvent is treated on an equal footing with the ions as a distinct molecular species. Our approach has been to extend the recent applications of the RHNC theory to bulk electrolyte solutions[1,2] by introducing an additional ionic component which is infinitely dilute and very much larger than the solvent molecules, and whose total charge may be adjusted to produce on its surface various charge densities of interest. The structure of the electrical double layer that forms about the curved surface of this macroion may then be derived from the correlation functions between it and the other species (cation, anion, and solvent) present in the solution.

In the first two papers[3,4] of this series we considered the response to the macroion of the solvent[3] and of single ions[4] at infinite dilution. In such an unscreened system the forms of these responses for a continuum solvent are known exactly, of course, and so the effects of the particulate nature of the solvent can be unambiguously identified. Although our electrolyte solution model is highly simplified—the ions, including the macroion, are charged hard spheres and the solvent molecules are hard spheres with embedded point multipoles of a magnitude and symmetry appropriate to liquid water—these results for infinite dilution are rich in solvent structural effects and have shown some novel but entirely plausible features. We summarize these briefly again here as they form the natural context in which to consider the new results for finite salt concentrations that we report in this paper.

With one important exception, the deviations of the macroion–solvent and macroion–ion correlation functions from the continuum solvent asymptotes are short ranged, extending no more than 8 Å or so from the surface. When the macroion diameter is 30 times that of a solvent molecule, the surface layers of solvent exhibit a very distinctive orientational order first observed and characterized by Lee *et al.*[5] in a molecular dynamics simulation of the ST2 model of water at a *flat* uncharged wall. This order arises as the system attempts to maximize the number of favorable intermolecular orientations between molecules in the contact layer and those in the immediately adjacent layers in a manner consistent with the high degree of orientational order of the bulk fluid. It can be somewhat loosely referred to as "ice-like" on account of the resulting similarity to ice I_h of the dominant contribution to the structure, although the fluctuations throughout the interface leave no doubt as to its essentially fluid nature. The highly directional character of the strong intermolecular forces seems to prevent the accommodation of this structure to surfaces that are only slightly more curved as our results for macroion diameters of 10 and 20 solvent diameters show only residual traces of the solvent structure at the flatter surface. These same strong intermolecular forces also turn out to be sufficient to preserve this structure at the flatter surface even in the electric field of quite substantial surface charges. The surface layers of solvent *are* polarized, of course, but only via a predisposition within the tetrahedral network established at the uncharged surface for orientations in which the component of the molecular dipole in the field direction is favorable. This has the very interesting consequence that the resulting solvent-mediated potential of mean force (PMF) between the macroion and an isolated small ion can be separated into a short-range and a long-range component. The former arises from the ion's response to the local solvent environment and, like that environment, is largely independent of surface charge; the latter, containing virtually all the charge dependence, arises

[a] Present address: Research School of Chemistry, Australian National University, Canberra, Australian Capital Territory 2601, Australia.

 0021-9606/89/084513-15$02.10 © 1989 American Institute of Physics

from the ion's response to the solvent polarization and assumes the continuum solvent result (i.e., Coulomb's law) until the separation is less than a molecular diameter from contact with the surface.

The exception to the stability of the solvent structure referred to above is the breakdown of this picture that occurs rather abruptly when the surface charge density reaches a value corresponding to about 120 Å^2 per electron. Beyond this value the solvent packing and polarization both develop pronounced oscillations which extend up to 30 Å from the surface; a similar change takes place at this point in the ion response as well.

Here we report the extension of these studies to systems in which a single macroion is immersed in a finite concentration salt solution and we investigate the effect of concentration on the response of both the solvent and the ion to the surface. Far from the surface the solvent polarization and the macroion–ion PMF will now assume the functional forms characteristic of an overall neutral system with electrostatic screening; of greater interest is the question of how salt concentration affects both solvent and ion structure close to the macroion surface. Although these short-range effects were found to be insensitive to the surface charge for any particular counterion at infinite dilution, in fact there was a great variety of behavior as the size of the small ion was changed.[4] In principle, then, a variety of different salts at finite concentration should be considered as well. We confine our attention in this paper, however, to KCl as a suitable prototype for which the *bulk* solution behavior as predicted by the RHNC theory is known to be fairly orthodox.[1]

II. MODEL, RHNC THEORY, AND NUMERICAL DETAILS

The electrolyte solution model that we use here is identical to that of Kusalik and Patey,[1] viz., hard sphere solvent molecules of diameter $d_s = 2.8$ Å with a point dipole μ and a tetrahedral point quadrupole of magnitude Θ, and monovalent hard sphere cations and anions of diameters d_+ and d_-, respectively. The bulk solution is characterized by the dimensionless parameters $\mu^* = \mu/\sqrt{d_s^3 kT}$, $\Theta^* = \Theta/\sqrt{d_s^5 kT}$, $\rho_s^* = \rho_s d_s^3$ and $\rho_+^* = \rho_-^* = \rho_+ d_s^3$ where ρ_s, ρ_+, and ρ_- are the number densities of solvent molecules, cations, and anions, respectively. The numerical values of these quantities are unchanged from the previous work on bulk solutions and for convenience we will designate each solution here simply by its molarity without repeating the specifications in terms of the dimensionless parameters given in Ref. 1. Into this bulk solution we introduce a single macroion as an additional ionic species of diameter d_m and charge Q.

The RHNC theory for the resulting mixture of four species is a straightforward application of the general RHNC theory of such systems described in detail in Ref. 1 and we limit ourselves here to a very brief description intended to give some idea of the computational resources required for the present problem.

The theory consists of the Ornstein–Zernike (OZ) equation

$$h_{\alpha\beta}(12) - c_{\alpha\beta}(12) = \frac{1}{8\pi^2} \sum_{\gamma}{}' \rho_\gamma \int h_{\alpha\gamma}(13) c_{\beta\gamma}(23) d(3) \tag{1}$$

and the RHNC closure relation,

$$c_{\alpha\beta}(12) = h_{\alpha\beta}(12) + c_{\alpha\beta}^{\mathrm{HS}}(r) - h_{\alpha\beta}^{\mathrm{HS}}(r) - \ln g_{\alpha\beta}(12) + \ln g_{\alpha\beta}^{\mathrm{HS}}(r) - u_{\alpha\beta}^{\mathrm{el}}(12)/(kT), \quad r \geqslant d_{\alpha\beta}, \tag{2}$$

$$h_{\alpha\beta}(12) = -1, \quad r < d_{\alpha\beta}.$$

In these equations the subscripts take the values s, $+$, $-$, and m denoting solvent, cation, anion, and macroion, respectively. The remaining symbols have their customary meanings: $h_{\alpha\beta}$, $c_{\alpha\beta}$, and $u_{\alpha\beta}^{\mathrm{el}}$ denote, respectively, the total and direct pair correlation functions and the electrostatic part of the pair potential between species α and β, $g_{\alpha\beta} = h_{\alpha\beta} + 1$, $d_{\alpha\beta} = (d_\alpha + d_\beta)/2$, and $d(3) = d\,\Omega_3 dr_3$ indicates integration over the position and orientational coordinates of particle 3. The superscript "HS" signifies a correlation function of the underlying hard sphere reference system for which we use the same parametrization as in our previous work,[3] suitably generalized to the present four species system.

The prime on the summation in Eq. (1) is a reminder that the term $\gamma = m$ is omitted since the macroion density ρ_m is zero; consequently, the subset of Eqs. (1) and (2) corresponding to $\alpha,\beta \neq m$ constitute the previously solved RHNC theory of the bulk electrolyte solution.[1] For the present system we need solve only the reduced set of Eqs. (1) and (2) in which $\alpha = m$ (using the correlation functions of the bulk electrolyte solution as input) to obtain the correlation functions involving the macroion component. This is accomplished through the expansion of the full correlation functions in a basis set of rotational invariants; this has been fully described elsewhere[1] and in what follows we use the notation of the previous work without further comment.

For the present four species system truncation of this expansion at $n_{\max} = 4$ results in a total of 105 projections to be included in the OZ equation at each step in the iterative procedure; of these, 95 are the fixed projections describing the bulk electrolyte solution and the remaining 10, the 2 ion density profiles and the 8 projections comprising the macroion–solvent radial distribution function, describe the double layer around the macroion. For most systems we use arrays of 2048 points for each projection giving a range of $40.94 d_s$ (115 Å), the exception being the $d_m = 10 d_s$ systems at 0.5 and 1.0 M where arrays half as large are sufficient. As with any completely numerical determination of the correlation functions of a system containing charged species careful attention must be paid to the preservation of overall electrical neutrality. The severest test in this regard among the systems we discuss here is posed by macroions of diameter $d_m = 30 d_s$ at 0.1 M for which the integration range mentioned above terminates at approximately 7 Debye lengths from the macroion–ion contact distance where $h_{m+}(r)$ is still $O(10^{-4})$. Even in this extreme case we found electroneutrality to be satisfied to better than 0.03% provided that the integration of the charge density is taken over all space including the hard core of the macroion. This latter qualifi-

cation is not important for neutral macroions or for charged macroions with $d_m = 10d_s$, but for charged macroions with $d_m = 30d_s$ we found convergence of $h_{m\pm}(r)$ to the exact value of -1 for $r < d_{m\pm}$ to be very sluggish. For such large particles there is a large volume element associated with distances just inside contact and so the charge arising from small imperfections in $h(r)$ in this region is not always negligible. When the same phenomenon occurred for macroions in the primitive model[6] the ultimate convergence of $h(r)$ to -1 inside the hard core could be pursued to completion but this required several thousand iterations. Although this is not practical for our systems (for the larger arrays a single iteration requires about 220 s on a FPS164 array processor) neither is it necessary as the rate of change of the correlation functions outside the hard core becomes imperceptible quite rapidly. In all cases we have extended the iterative process until the charge arising from the residual imperfections in $h(r)$ inside contact is less than 2% of the macroion charge, typically 200 to 400 iterations, but this is well past the point at which further changes would be visible on any of the figures that we show in the following section.

III. RESULTS AND DISCUSSION

In our previous work[3,4] we considered macroion diameters d_m of $10d_s$ (28 Å), $20d_s$ (56 Å), and $30d_s$ (84 Å). Those earlier calculations demonstrated that the structure of the interfacial region depends critically on the degree of curvature of the macroion surface, with the macroion of diameter $30d_s$ inducing planar-like behavior that is qualitatively different from the other two cases. Accordingly, we consider in the following discussion the two extremes $d_m = 30d_s$ and $d_m = 10d_s$. For consistency with the earlier work, however, we continue to describe the surface charge density σ for all systems in terms of the number of elementary charges required to produce it on the surface of a macroion with diameter $20d_s$. We report results here for the same set of negative surface charge densities as before, viz., $\sigma = 0$, -28, -56, and -108; the largest of these corresponds to about -0.175 C m^{-2} or 91 Å^2 per electron. The symmetric solvation property of the tetrahedral solvent model we are using here admits a second equivalent description of the theoretical results in which the charge of each ionic species and the dipole moment of the solvent are all reversed. In the model for KCl, however, the cation and anion diameters are slightly different ($d_+ = 1.08d_s$, $d_- = 1.16d_s$) so that the exact determination of the double layer properties of this salt in the presence of a positively charged macroion would require separate calculations for such systems. We report here results only for $\sigma \leqslant 0$, though, because the solvent is not very sensitive to such small differences in the ionic diameters and we expect the properties of the double layer in this particular system to be nearly antisymmetric about $\sigma = 0$ with a very small potential of zero charge (pzc). We hasten to add, however, that KCl in the tetrahedral solvent is exceptional in this regard and that either greater asymmetry in the ion diameters or a more refined model of the solvent would produce a substantial dependence on the sign of the macroion charge.

Our previous calculations were limited to zero concentration of electrolyte where the solvent response to the macroion is unaffected by the infinitely dilute counterions and coions. Although this simplification does not extend to the finite concentration case under consideration here where the solvent and ion behaviors are coupled, the division into ionic and solvent response remains a natural way to organize the discussion of the interfacial structure.

A. Ionic structure in the interface

The solid lines in Fig. 1 are the RHNC results for Φ_{m+} the potential of mean force between the macroion and a potassium counterion K^+ for various surface charge densities on a macroion of diameter $30d_s$ in 0.1 M KCl. (The potentials of mean force in this and all subsequent figures are expressed in units of kT.) Φ_{m+} and Φ_{m-} have their usual definitions in terms of the more customary radial distribution functions or relative density profiles,

$$\Phi_{m\pm}(r) \equiv -kT \ln g_{m\pm}(r) \tag{3}$$

but we use the former here to facilitate comparison with our previous results at infinite dilution and to mitigate the difficulties of displaying the rapidly varying $g_{m+}(r)$ near contact for highly charged surfaces. The broken lines in this figure show the results of fitting $\Phi_{m+}(r)$ far from the surface to the assumed asymptotic form

$$\Phi_{m+}(r) \sim A_{m+} e^{-\kappa r}/r, \tag{4}$$

where, as we would expect, the screening parameter κ agrees with that characterizing the RHNC results for the long-range correlations in the bulk solution (and is therefore different,[1] in general, from the Debye parameter κ_D) and the constant A_{m+} depends on the nature of the macroion and the counterion as well as on the bulk solution. The insets in each panel of this figure show the analogous results for the potential of mean force between the macroion and the K^+ species at infinite dilution. (In this case the asymptotic form of $\Phi_{m+}(r)$, being simply Coulomb's law, has the status of an exact result unlike Eq. (4) which has only been shown to be exact in the low concentration limit.)

The obvious feature of the Φ_{m+} for moderate surface charges in Fig. 1(a)–1(c) is the striking resemblance of the results at 0.1 M to those at infinite dilution even after allowance is made for the coarser vertical scales needed to display the infinite dilution results. In both cases, the asymptotic behavior of a continuum solvent model is reached within four molecular diameters of the surface and the fine structure within $4d_s$ of the surface, representing the influence of the local structure of the molecular solvent on the ionic response to the surface, shows almost no concentration effect at all. This is entirely consistent with the picture of the interfacial region that we had built up based on the RHNC results at infinite dilution.[3,4] There, even without the attenuation arising from ionic screening, the electric field of the macroion had little effect on the intermolecular correlations in the surface layers of solvent and hence the effect of the molecular nature of the solvent on the macroion–ion potential of mean force was short ranged and nearly independent of surface charge. This was certainly not the case at high sur-

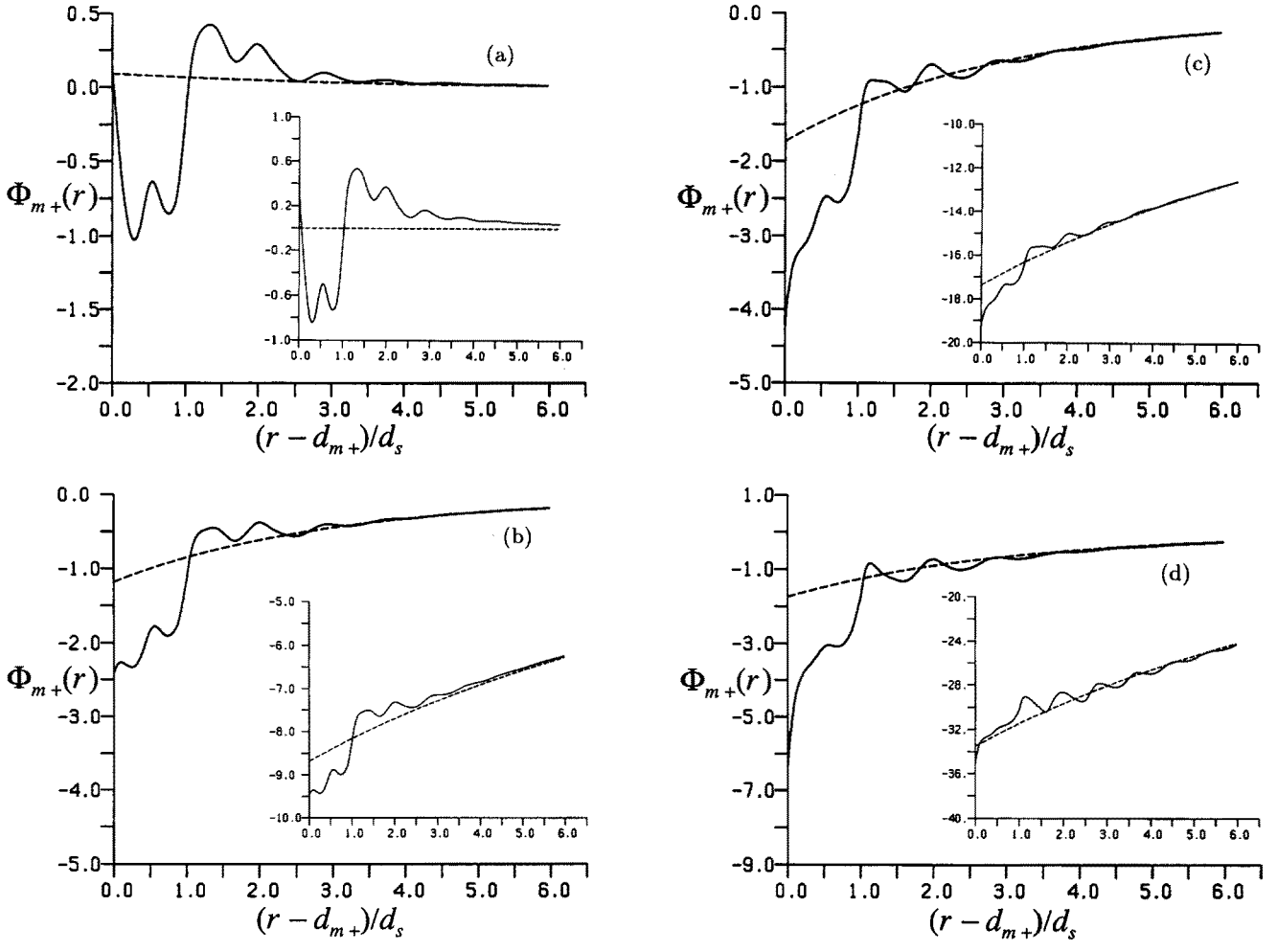

FIG. 1. Potential of mean force Φ_{m+} between a $30d_s$ macroion and a counterion K^+ for various surface charge densities σ in 0.1 M KCl; (a) $\sigma = 0$; (b) $\sigma = -28$; (c) $\sigma = -56$; (d) $\sigma = -108$. (—) $\Phi_{m+}(r)$; (– –) asymptote of Φ_{m+} [cf. Eq. (4)]. The insets show Φ_{m+} and its Coulomb law asymptote at infinite dilution for the same surface charges. (Note: in all figures Φ is expressed in units of kT.)

face charges, however, where a substantial layering of the solvent density could be induced accompanied by marked oscillations in both the polarization and Φ_{m+} extending well out into the solvent. This is precisely the case for which noticeable differences between the 0.1 M and infinite dilution Φ_{m+} are evident in Fig. 1(d). (The visual impact of these differences in this figure is diminished somewhat by the coarse vertical scale needed for the inset, as mentioned above.) The first of these differences is a pronounced negative deviation of Φ_{m+} from the continuum asymptote at 0.1 M that forms part of a smooth trend evident in Figs. 1(a)–1(c) yet is absent from the infinite dilution Φ_{m+} at the same high surface charge. Second, the finite concentration Φ_{m+} for $\sigma = -108$ does not exhibit the long-range oscillatory behavior of the infinite dilution result. This is a screening effect of the counterions, of course, but not one that should be thought of in terms of the conventional continuum solvent picture in which such screening takes place on a distance scale characterized by the bulk solution parameter κ. This we demonstrate by a consideration of the quantity $f_Q(r)$ the fraction of the total macroion charge Q that has been neutralized by mobile ions within a distance r of the center of the macroion,

$$f_Q(r) \equiv -4\pi/Q \int_{d_{m+}}^{r} [q_+\rho_+(s) + q_-\rho_-(s)]s^2\,ds. \quad (5)$$

If the asymptotic form of $h_{m\pm}$ consistent with that for Φ_{m+} in Eq. (4), namely $h_{m\pm} \sim e^{-\kappa r}/r$, held for all $r > d_{m+}$ then $f_Q(r)$ would be given by

$$f_C(r) = 1 - e^{-\kappa(r-d_{m+})}(r+\kappa^{-1})/(d_{m+}+\kappa^{-1}) \quad (6)$$

independent of Q. In Fig. 2 we show $f_c(r)$ (solid line) and $f_Q(r)$ for each of the charged macroions of Figs. 1(b)–1(d). Clearly, there are two distinct regions of ionic screening in these systems separated by a remarkably sharp boundary at one molecular diameter from contact with the surface. A fit of the quantity $1 - f_Q(r)$ to $Bre^{-\alpha r}$ confirms that continuum solvent-like behavior (i.e., $\alpha = \kappa$) of the screening is established almost immediately beyond this boundary.

The behavior of $f_Q(r)$ close to the surface is more complex, arising as it does from several competing effects. The most obvious of these, and the dominant effect for highly charged surfaces, is the direct Coulomb attraction felt by the counterions in contact, or near contact, with the surface where neither solvent molecules nor other counterions can

directly intervene to contribute to the screening. This effect accounts for the deep attractive well near contact in Figs. 1(c) and 1(d) and is extraordinarily large; e.g., at $\sigma = -108$ nearly 80% of the macroionic charge has been neutralized by counterions situated within one diameter of contact with the surface. Even at this our largest macroionic charge, the surface *number* density of charges is still low; as a result, there is always ample room for solvent molecules to mediate the lateral repulsions among the counterions in this contact layer. Consequently, this "fast screening" effect becomes larger in relative terms with increasing surface charge as shown in Fig. 2. In fact, this relative increase in the fast screening within one diameter of contact in passing from $\sigma = -56$ to $\sigma = -108$ turns out to neutralize exactly all of the additional macroionic charge in the $\sigma = -108$ system. That is, for both these surface charge densities the actual *net* charge accumulated up to the evident break in $f_Q(r)$ at one diameter from contact is the same (to within 1%) and corresponds to $\sigma \doteq -24$. As a result, beyond this region the response of the solution (both the solvent polarization and the charge density) is essentially the same for both systems even though Q has more than doubled. This suggests the existence of a maximum *effective* surface charge density that any given electrolyte concentration can support but we have too little data to decide the generality of this very interesting phenomenon.

This rapid neutralization also accounts for the lack of a qualitative change at high surface charge in Φ_{m+} at finite concentration, in contrast to the behavior of Φ_{m+} at infinite dilution. As $|\sigma|$ increases the resulting growth in polarization of the surface layer of solvent will make a contribution to the local field close to the surface that is unfavorable to counterions in the contact layer. At infinite dilution this develops unchecked by ionic screening leading to the qualitative change in the solvent structure at $\sigma = -108$ and the attenuation of the attractive well in Φ_{m+} evident in the inset of Fig. 1(d). At finite concentration, however, the fast screening described above prevents the effective field experienced by the solvent from reaching the values needed to bring this about and the results in Fig. 1(d) for 0.1 M show instead a smooth continuation of the trends visible at lower surface charges.

In addition to these rather direct electrostatic effects $f_Q(r)$ will, in general, also reflect the short-range structure in $\Phi_{m\pm}$ which we associate with the response of the ion to the ice-like orientational structure of the solvent surface layer. This structure in $\Phi_{m\pm}$ is generally a very sensitive function of the ion diameter[4]; for K^+ it takes the form of a shallow attractive well near contact with a double minimum [cf. Fig. 1(a)] though the nearer minimum is eventually washed out by the direct attractive effect at contact at higher charges [Figs. 1(c) and 1(d)]. The effect on $f_Q(r)$ of this type of deviation from the asymptotic PMF will depend primarily on the *difference* between the individual cation and anion discrepancies of this type. These happen to be small for our nearly identical K^+ and Cl^- ions so that the additional screening effect that might be expected on the basis of the extra attractive well in Φ_{m+} is largely offset by a similar well in Φ_{m-}. However, the situation would likely be quite different for a less symmetric salt such as NaCl or CsF.

However, the small differences in the solvent structural effects on the short-range part of Φ_{m+} and Φ_{m-} that do exist for KCl are interesting in their own right and are helpful in illustrating the role of the molecular solvent in controlling the ionic response to the surface. These effects are most evident at the uncharged surface and hence we digress briefly here to discuss the details of the ionic structure for $\sigma = 0$. Upon close inspection Φ_{m+} in Fig. 1(a) will be seen to have a weak repulsive asymptote described by Eq. (4) and which arises at this neutral surface from a small positive charge separation in the ionic structure. (The associated positive pzc is extremely small as our introductory discussion anticipated.) The slightly smaller K^+ species of our model can approach the surface more closely than Cl^- and it would be natural to suppose that this direct effect accounts for the sign of the charge separation, as indeed it does in a continuum solvent model.[7] In the molecular solvent, however, there is a second more subtle but larger effect that is revealed when the density profiles for both cations and anions are plotted together, as in Fig. 3. The real source of the charge separation close to the surface is the existence of a much larger *second*

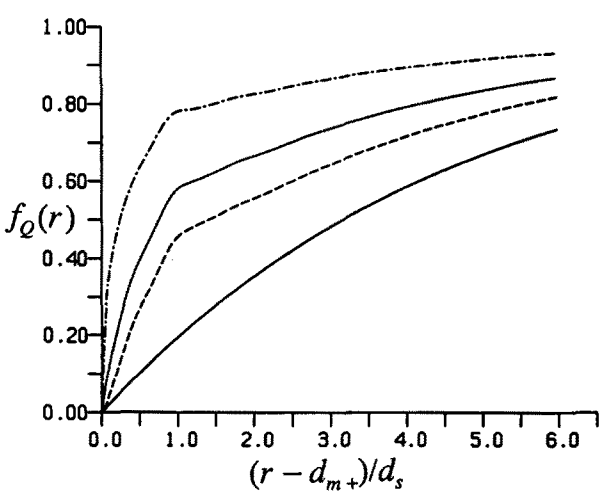

FIG. 2. Fractional charge profile $f_Q(r)$ [Eq. (5)] for double layers at a $30d_s$ macroion in 0.1 M KCl. (– –) $\sigma = -28$; (···) $\sigma = -56$; (–·–·) $\sigma = -108$; (—) "continuum" result $f_c(r)$, Eq. (6).

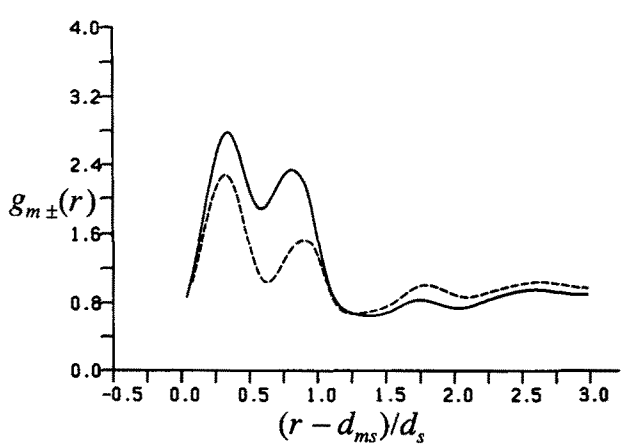

FIG. 3 Ion density profiles $g_{m+}(r)$ next to an uncharged $30d_s$ macroion in 0.1 M KCl. (—) $g_{m+}(r)$; (---) $g_{m-}(r)$.

density peak in $g_{m+}(r)$ than in $g_{m-}(r)$ near $0.7d_s$ from contact. This second peak is fine structure, to be sure, and difficult to rationalize from the structural information produced by our solution of the homogeneous OZ equation. The point we wish to make here is that the charge separation at the surface has arisen through a discrimination of the ions by the local structure of the molecular solvent rather than from the differences in the direct ion–surface interactions. It is still an ion size effect in the sense that the tetrahedral solvent would not differentiate at all between cations and anions of equal size and it is a measure of the great sensitivity of solvation effects to ion size that the very small difference between d_+ and d_- in KCl can lead to the substantial differences in the profiles in Fig. 3. Similar effects would be much greater for other salts having a greater size asymmetry between cation and anion.

Except at neutral surfaces like the foregoing, the role of coions in the interface is of little consequence and we focus in what follows exclusively on the counterion structure. In considering our earlier results for Φ_{m+} at infinite dilution,[4] we found it useful to introduce the excess quantity

$$\Phi^{ex}_{m+}(r) \equiv \Phi_{m+}(r) - Qq_+/(\epsilon r) \tag{7}$$

which was short ranged and almost completely independent of the macroion charge Q. The strong resemblance of the Φ_{m+} at 0.1 M in Fig. 1 to the infinite dilution Φ_{m+} in the insets obviously suggests the definition of a similar quantity at finite concentration in terms of the numerically measured asymptote of Eq. (4),

$$\Phi^{SR}_{m+}(r) \equiv \Phi_{m+}(r) - A_{m+}e^{-\kappa r}/r. \tag{8}$$

In Fig. 4(a) we reexpress the information of Fig. 1 using these short-range quantities. Those in the inset are typical of our earlier results for other ions at infinite dilution[4]: for $|\sigma| \leqslant 56$ Φ^{ex}_{m+} has no charge dependence except within $0.2d_s$ of contact, whereas the qualitative change at $\sigma = -108$ is emphasized in the excess quantity. It would be surprising if the ionic screening at finite concentrations *increased* the charge dependence of the short-range behavior and, in fact, the Φ^{SR}_{m+} for 0.1 M in this figure also have very little variation with σ except very close to contact. This observation now applies as well to the previously exceptional case of $\sigma = -108$ because the fast ionic screening itself prevents the drastic changes in the solvent structure that determined the infinite dilution Φ^{ex}_{m+}.

Consistent with this insensitivity to surface charge is a similar insensitivity of these short-range functions to concentration as well, evident in the comparison of Φ^{SR}_{m+} to Φ^{ex}_{m+} in Fig. 4(a). Our results for Φ^{SR}_{m+} for these same macroions remain unchanged from those at 0.1 M in this figure when the concentration is increased to 0.5 M. At still higher concentrations the screening length κ^{-1} becomes comparable to the distances characterizing the short-range solvent structural effects and the asymptotic component of Φ_{m+} implied by Eq. (4) can no longer be accurately detected numerically (this is also true of the correlations between small ions in the bulk solution[1]). By 1.0 M, the *full* Φ_{m+} shown in Fig. 4(b) is itself a short-range function, but one that remains almost identical to the short-range quantity Φ^{SR}_{m+} at lower concentrations as a comparison with Fig. 4(a) shows. As the concentration increases the deep well in Φ^{SR}_{m+} at contact changes little and therefore has an increasing amount of charge associated with it. Consequently, the cumulative charge profile $f_Q(r)$ is a strong function of concentration. At 1.0 M, $f_Q(r)$ shown in Fig. 5 is no longer monotonic, with a maximum for all surface charges occurring near one diameter from contact, the same distance at which the curvature of $f_Q(r)$ changes so abruptly at lower concentrations. At this point there is an excess neutralization of as much as 20% of the surface charge and the response of the system beyond this point will be characteristic of that for a less highly charged *positive* surface.

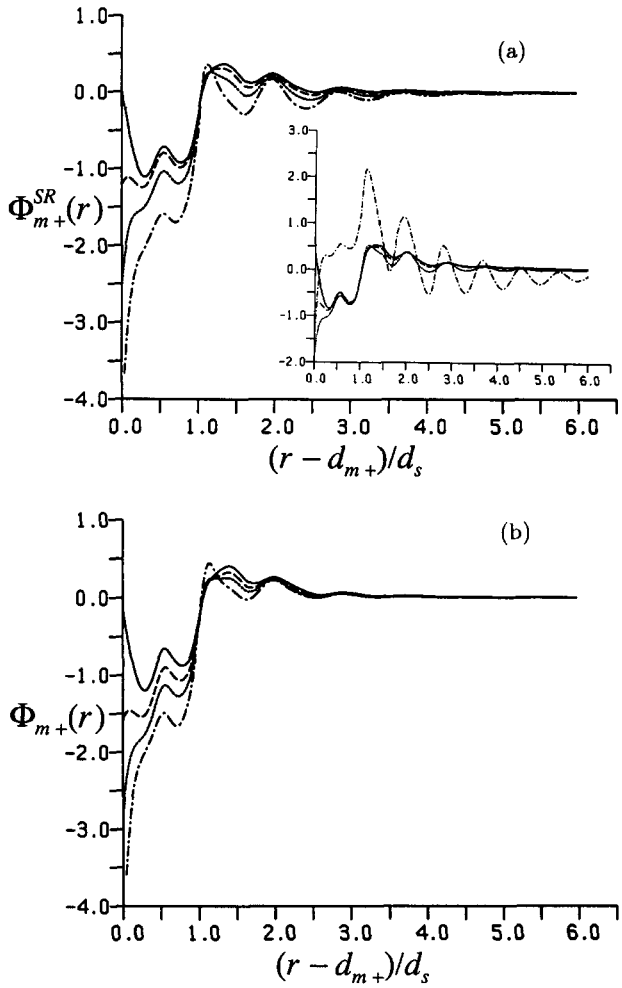

FIG. 4. (a) Short-range potential of mean force Φ^{SR}_{m+} [Eq. (8)] between a $30d_s$ macroion and a K^+ counterion in 0.1 M KCl for various surface charges. (—) $\sigma = 0$; (– –) $\sigma = -28$; (···) $\sigma = -56$; (–·–·) $\sigma = -108$. The inset shows the analogous quantity Φ^{ex}_{m+} [Eq. (7)] at infinite dilution. (b) As for (a), but in 1.0 M KCl. Note that here the function shown is the total potential of mean force Φ_{m+}.

For smaller macroions the Φ_{m+} are quite different. This is because the high degree of orientational order characterizing the solvent structure at a flat surface cannot be established at more highly curved surfaces. Generally, the response of small ions to this change in the solvent

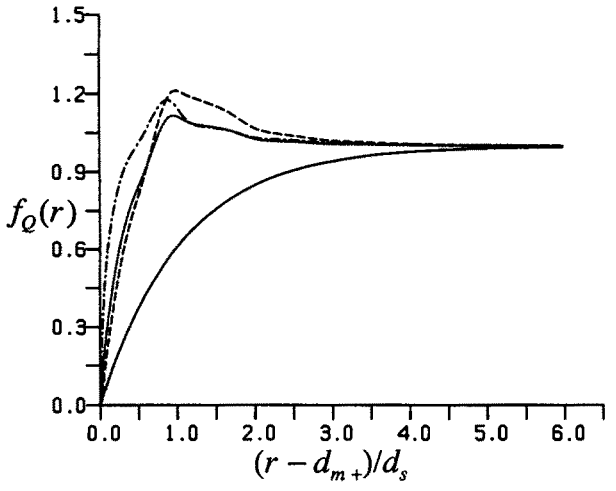

FIG. 5. Fractional charge profile $f_Q(r)$ for double layers at a $30d_s$ macroion in 1.0 M KCl. Symbols as in Fig. 2. The screening parameter κ used to calculate $f_c(r)$ in this figure is approximate, based on examination of the RHNC results for bulk 1.0 M KCl (Ref. 1).

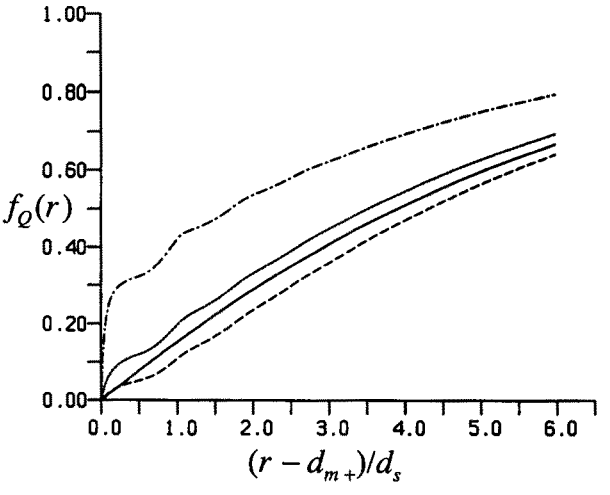

FIG. 7. Fractional charge profiles $f_Q(r)$ and $f_c(r)$ for double layers at a $10d_s$ macroion in 0.1 M KCl. Symbols as in Fig. 2.

environment near the more highly curved surface is a sensitive function of the small ion size.[4] However, for ions such as K^+ that are not too large and therefore interact strongly with the solvent, the *short-range* quantity Φ^{SR}_{m+} shows an extra attractive effect in the highly ordered solvent layer for $d_m = 30d_s$ (cf. the well near $0.6d_s$ in Fig. 1) but is repulsive instead near moderately charged smaller macroions. An example of this is evident in Fig. 6 where we plot Φ^{SR}_{m+} for a macroion with $d_m = 10d_s$ and the same set of surface charge densities used in Fig. 1 for $d_m = 30d_s$. For high surface charges the attractive well at contact is inevitable and produces the same fast screening that typified the results for $d_m = 30d_s$ in Fig. 2, but for lower surface charges the repulsion referred to above actually inhibits the screening. This is illustrated in Fig. 7 where the fractional charge profile $f_Q(r)$ for $\sigma = -28$ lies below that given by the "continuum" result of Eq. (6). Even the fast screening for $\sigma = -108$ is inhibited to some extent by this repulsive component of Φ^{SR}_{m+} as "only" 40% neutralization is realized for the smaller macroion within one diameter of contact compared to 80% when $d_m = 30d_s$.

B. Solvent structure in the interface

Even for a neutral macroion, there will be small effects on the solvent response to the surface arising from the presence of a finite concentration of electrolyte. Ionic screening obviously will reduce the range of solvent–solvent correlations; eventually this becomes sufficient to have a discernible impact on the hydrophobicity of the neutral macroion as measured by the solvent–macroion radial distribution function $g_{ms}(r)$. This quantity is shown in Fig. 8 for a macroion of diameter $d_m = 30d_s$ in KCl solutions of varying concentrations up to 4.0 M. There is a large effect only at the highest concentration where the polar nature of the solvent has been moderated sufficiently that $g_{ms}(r)$ shows a tendency near contact to become more "hard sphere-like" although there is still a maximum in the density at $0.1d_s$ from contact. The

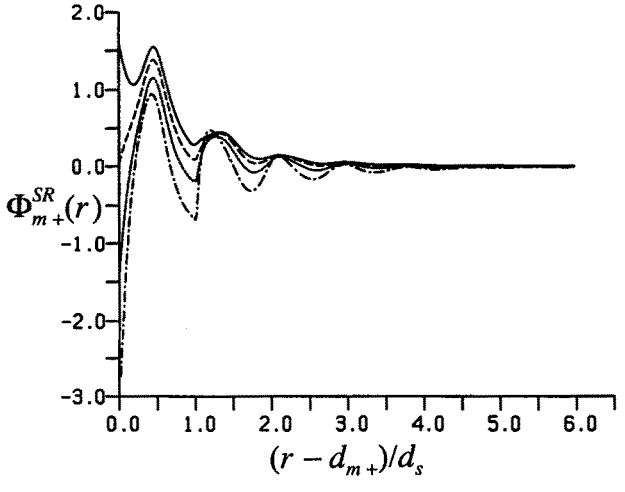

FIG. 6. Short-range potential of mean force Φ^{SR}_{m+} between a $10d_s$ macroion and a K^+ counterion in 0.1 M KCl, all symbols as in Fig. 4.

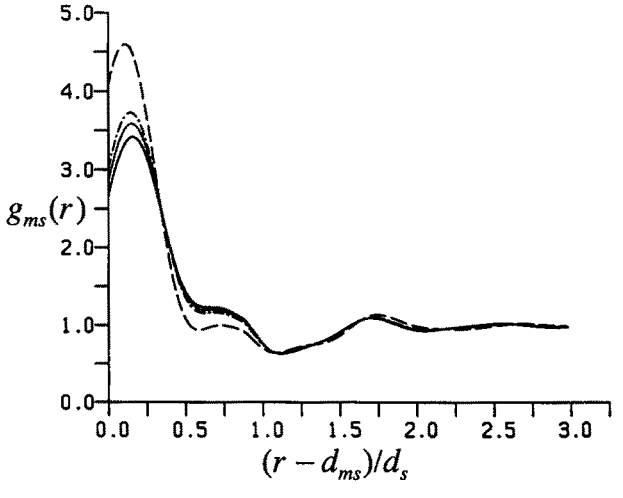

FIG. 8. Solvent density profile $g_{ms}(r)$ next to an uncharged $30d_s$ macroion in various concentrations of KCl. (—) infinite dilution; (···) 0.5 M; (–·–·) 1.0 M; (– –) 4.0 M.

orientational structure of the solvent in the interfacial region is largely controlled by the short-range forces between solvent molecules, however, and at this neutral surface is not expected to be sensitive to the bulk salt concentration. This is confirmed in Fig. 9 where we show the concentration dependence for these same systems of the quantity $P_2(\cos\theta_\mu)$, the second Legendre polynomial of the cosine of the angle between the dipole of a solvent molecule and the surface normal. Despite the 30% increase in the local density at 4.0 M shown in Fig. 8, the well in P_2 characteristic of the orientational order in the surface layer of solvent at infinite dilution is essentially unchanged by concentration.

A quite separate effect of concentration on the local solvent structure arises from the slight asymmetry between the cation and anion in KCl. We have already shown in Fig. 3 how this leads to a small positive charge separation at a neutral surface in 0.1 M KCl. This will polarize the solvent—a symmetry-forbidden phenomenon for the *pure* tetrahedral solvent at a neutral surface—but again the effect is scarcely discernible until the concentration reaches 4.0 M. To illustrate it we reintroduce the function $p(\theta)$, the probability density for the angle between the surface normal and either the molecular dipole (θ_μ) or the OH bond (θ_{OH}) for solvent molecules at a given distance from the surface.[3] In Fig. 10 we show $p(\theta_\mu)$ for the pure solvent, 1.0 and 4.0 M KCl for molecules in contact with a neutral surface [Fig. 10(a)] and at a distance of $0.66d_s$ from the surface [Fig. 10(b)]. The pure solvent results (solid lines) are taken from Figs. 2(a) and 2(c) of Ref. 3 and are necessarily symmetric about 90°. This symmetry is broken for the finite concentration systems in a manner consistent with the charge separation implied by the ion density profiles in Fig. 3: a slight favoring of dipole orientations towards the surface (large angles) for molecules in the contact layer and a corresponding enhancement of orientations away from the surface for molecules lying just outside the region of positive charge. This is yet another example of an effect that is likely to be unusually small for the nearly symmetric KCl so it is particularly pleasing to see that the theory has nevertheless made a plausible prediction of such a subtle phenomenon.

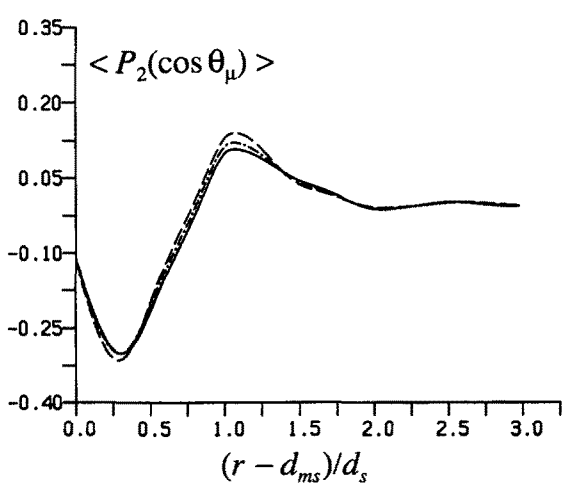

FIG. 9. Order parameter $P_2(\cos\theta_\mu)$ for solvent next to an uncharged $30d_s$ macroion in various concentrations of KCl. Symbols as in Fig. 8.

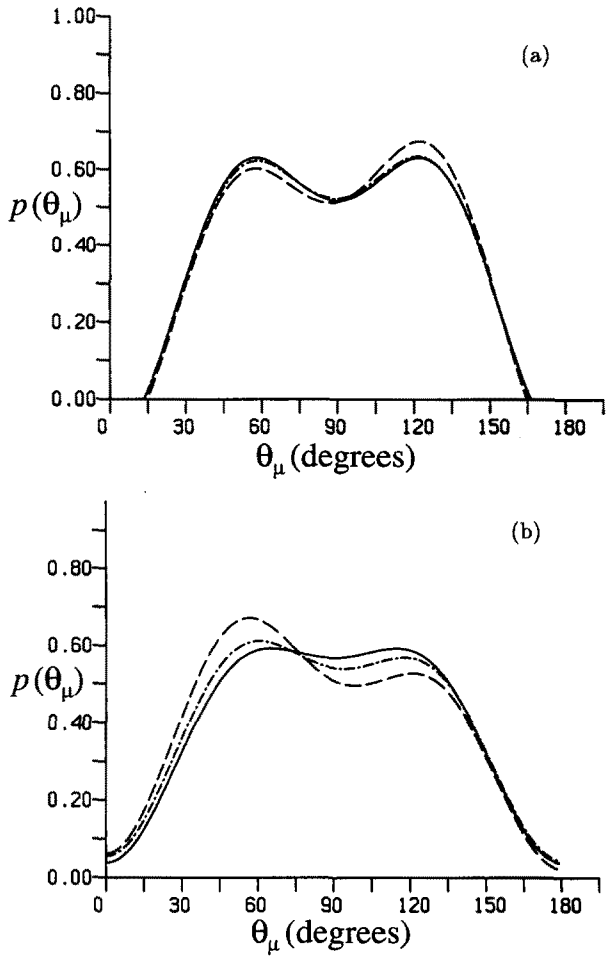

FIG. 10. Probability density $p(\theta_\mu)$ for solvent molecules at a distance r from contact with an uncharged $30d_s$ macroion in various concentrations of KCl. Symbols as in Fig. 8. (a) $r = 0$; (b) $r = 0.66d_s$.

Two features dominate the behavior of the pure solvent near a charged surface.[3] The first of these is the dramatic and abrupt qualitative change in the solvent structure at high surface charge to a slowly decaying oscillatory response in both the packing density and the polarization that extends out many diameters from the surface. This we believe to be a consequence of achieving a coupling of the surface field to the molecular dipoles that is strong enough to overcome the ordering due to the highly directional intermolecular forces in the solvent. The results for Φ_{m+} described above have already made clear that there is no such long-range oscillatory structure in any of the finite concentration systems we have considered here and the fractional charge profiles $f_Q(r)$ in Figs. 2 and 5 show why this is so. The high surface charge is neutralized so rapidly by a large concentration of counterions in contact with the surface that even solvent molecules very close to the surface experience a much smaller effective field that is well below the strength required to cause the oscillatory phenomena in the pure solvent. As a result, the solvent packing at $\sigma = -108$ shown in Fig. 11 has a negligible concentration dependence over the range 0.1–1.0 M just as the packing in the pure solvent has little *charge* dependence for $|\sigma| \leqslant 80$.[3] Because this fast screening does not ap-

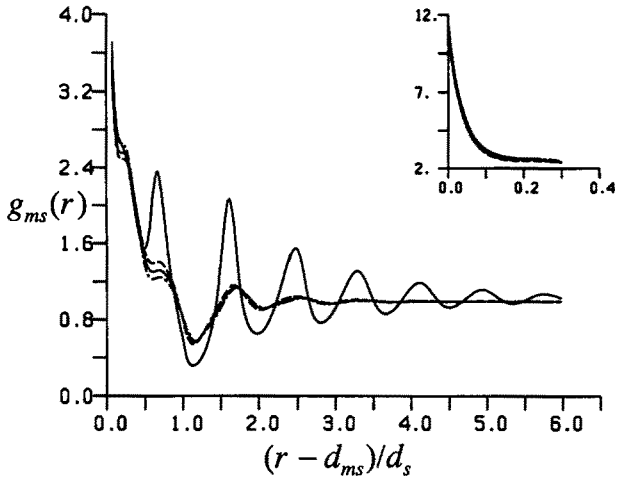

FIG. 11. Solvent density profile $g_{ms}(r)$ next to a $30d_s$ macroion with $\sigma = -108$ for various KCl concentrations. (—) infinite dilution; (– –) 0.1 M; (···) 0.5 M; (–·–·) 1.0 M.

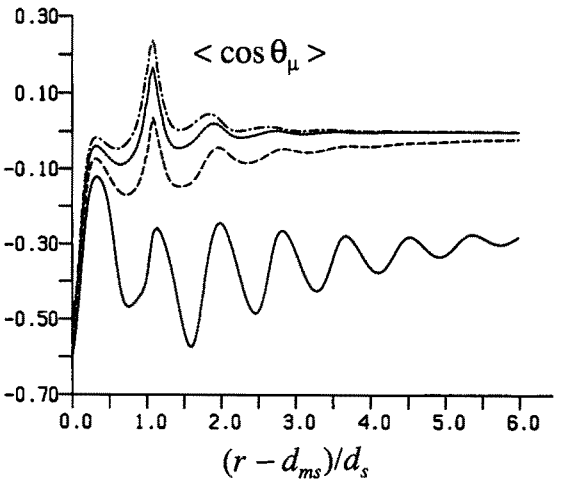

FIG. 12. Mean polarization per solvent particle $\langle \cos \theta_\mu \rangle$ for solvent near a $30d_s$ macroion with $\sigma = -108$ for various KCl concentrations. Symbols as in Fig. 11.

pear to operate on a concentration-dependent distance scale, the relevance to finite concentration systems of the oscillatory structure in the pure solvent at large σ in Fig. 11 is an open question. There is no known rigorous low concentration limiting behavior that is independent of σ to guide us and the suggestion in the 0.1 M results of the existence of a rather low limit to the effective macroionic charge could mean that the field necessary to induce this structure cannot be sustained at any reasonable finite value of the salt concentration. However, the concentration range we have explored here is still too high to resolve this point.

These same observations apply to the pure solvent result for the profile of the mean polarization per particle $\langle \cos \theta_\mu \rangle$ in Fig. 12 (solid line) for $\sigma = -108$ and we proceed directly to a discussion of the finite concentration results for $\langle \cos \theta_\mu \rangle$ in this figure. The notable feature is a narrow peak centered at $1.08d_s$ from contact, corresponding to solvent molecules separated from the surface by the layer of positive counterions in contact with the macroion. At the higher concentrations where the charge in this initial contact layer of counterions actually exceeds the macroion charge (cf. Fig. 5) this peak in the polarization is positive and $\langle \cos \theta_\mu \rangle$ decays to zero from above. The behavior at 0.1 M is more conventional and the long-range screening of the negative tail in $\langle \cos \theta_\mu \rangle$ ($\sim -e^{-\kappa r}/r^2$) is clearly visible beyond the region of short-range structure. At lower surface charges the polarization profiles are less dramatic than those in Fig. 12 (and the pure solvent results no longer oscillatory) but the feature at $1.08d_s$ is still clearly present for all the finite concentration systems.

The second feature of the pure solvent surface structure is, of course, the ordering of the contact layers into an ice-like arrangement for $d_m = 30d_s$ and the subsequent immunity of the molecular arrangements in this layer to the surface charge. The signature of this structure is an inversion in the shape of the angular probability density $p(\theta_{OH})$ between molecules in contact with the surface and those about 1.8 Å from contact [Figs. 1(a) and 1(c) of Ref. 3]. For a neutral surface we find *no* significant concentration effect on the $p(\theta_{OH})$ measured previously for the pure solvent.[3] The concentration dependence of $p(\theta_{OH})$ at high charge, shown in Fig. 13, is more interesting. For solvent molecules in contact with the surface [Fig. 13(a)] there is again no significant change in $p(\theta_{OH})$ with concentration; these molecules are directly exposed to the bare Coulombic field of the macroion whatever the salt concentration in the bulk solution. For solvent at a distance of $0.66d_s$ from contact, on the other hand, the restoration of the peak in $p(\theta_{OH})$ at zero degrees with increasing concentration in Fig. 13(b) is strongly evocative of the trend in $p(\theta_{OH})$ with decreasing *charge* for the pure solvent in Fig. 6(c) of Ref. 3. There is an equally remarkable resemblance between the concentration dependence of the dipole angle distribution $p(\theta_\mu)$ at this same distance, shown in Fig. 14(b), and the variation of $p(\theta_\mu)$ with charge in the pure solvent, shown in Fig. 7(c) of Ref. 3. Again, $p(\theta_\mu)$ for molecules in contact with the surface [Fig. 14(a)] is relatively insensitive to concentration.

A relatively simple picture emerges, then, of the influence of concentration on the solvent orientational order in the interface. The rapid neutralization of the surface charge by counterions in contact or nearly in contact with the surface causes all but the contact solvent molecules to experience the electric field of a substantially lower effective surface charge; the higher the concentration the greater this rapid screening and the lower the effective charge. The tetrahedral coordination between solvent molecules that characterizes the ice-like surface structure is destroyed neither by surface charge nor by salt concentration, the solvent polarization takes place within this structure as we described previously[3] and is diminished by rapid counterion screening at finite concentration to a level commensurate with the response of the pure solvent to a lower effective surface charge.

C. The electrostatic potential

Our primary focus in this work has been on the microscopic structure of the charged interface. This, however, is generally not directly accessible experimentally and so we

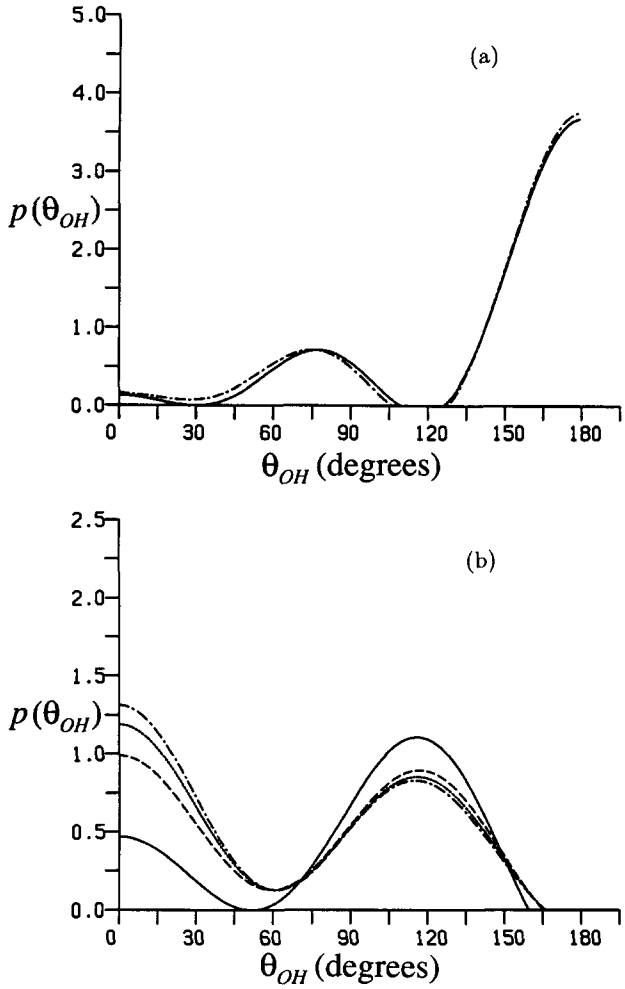

FIG. 13. Probability density $p(\theta_{OH})$ for solvent molecules at a distance r from contact with a $30d_s$ macroion with $\sigma = -108$ in various concentrations of KCl. Symbols as in Fig. 11. (a) $r = 0$; (b) $r = 0.66d_s$.

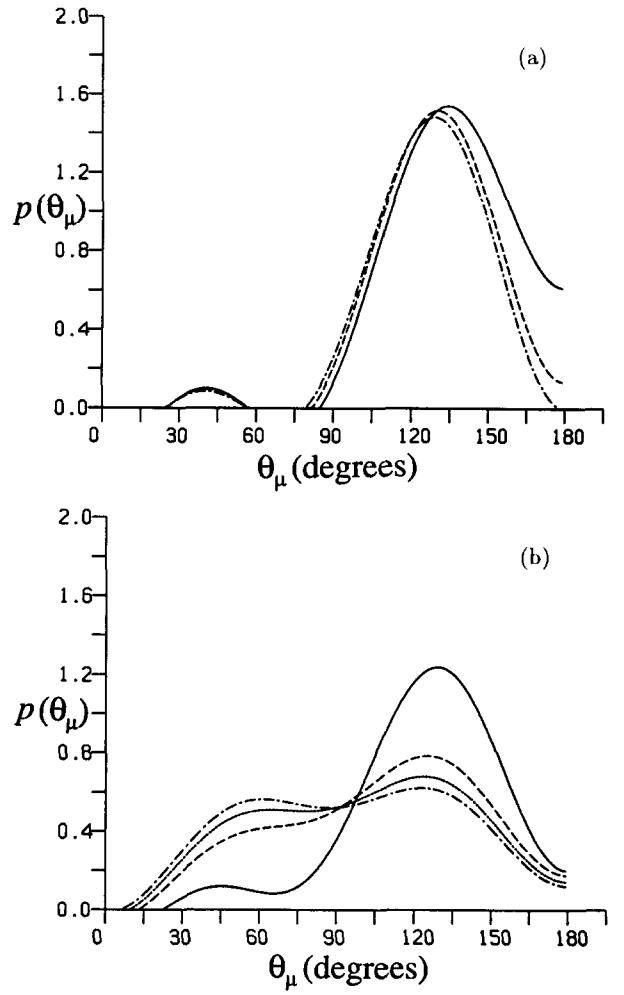

FIG. 14. Probability density $p(\theta_\mu)$ for solvent molecules at a distance r from contact with a $30d_s$ macroion with $\sigma = -108$ in various concentrations of KCl. Symbols as in Fig. 11. (a) $r = 0$; (b) $r = 0.66d_s$.

turn our attention here to the implications of structure such as we have been describing for observable properties of the double layer. Of special importance is the differential capacitance C_D because its behavior in dilute solution[8] is the foundation for the widespread conceptual division of the interface into an outer diffuse layer described by Gouy–Chapman theory and an inner layer dominated by short-range interactions of the solvent molecules and counterions with the surface.[9] C_D is defined by $C_D \equiv d\sigma/d\Psi_s$ where $\Psi_s = \Psi(d_m/2)$ is the electrostatic potential on the surface relative to zero in the bulk solution, i.e., the potential drop across the interface. $\Psi(r)$ is given by

$$\Psi(r) = \Psi_{\text{ionic}}(r) + \Psi_{\text{solv}}(r)$$
$$= Q/r + 4\pi/r \int_0^r [q_+\rho_+(s) + q_-\rho_-(s)]s^2\,ds$$
$$+ 4\pi \int_r^\infty [q_+\rho_+(s) + q_-\rho_-(s)]s\,ds$$
$$- \frac{4\pi\rho_s\mu}{3} \int_r^\infty h_{00}^{011}(s)ds$$
$$+ 4\pi\rho_s\Theta \frac{8}{5\sqrt{6}} \int_r^\infty \frac{h_{02}^{022}(s)}{s}\,ds. \tag{9}$$

The cancellation between the ionic terms and the solvent response which produces a net potential that is only $O(1/\epsilon)$ of either component must be carried out numerically in a theory such as we have used here. A vivid impression of the problem this poses for the present model ($\epsilon \doteq 93.5$) is given by Fig. 15(a) which shows both contributions to $\Psi(r)$ and the resulting total potential for a typical case, $d_m = 30d_s$, $\sigma = -56$ in 0.1 M KCl. The total ionic contribution (solid line) passes smoothly across the hard core boundaries in accordance with the electrostatic boundary condition for the electric displacement. The reaction field of the solvent (broken line), on the other hand, rises very steeply just before the contact distance reflecting the high degree of polarization of solvent molecules in the contact layer as they respond to the bare unscreened field of the macroion. (This is

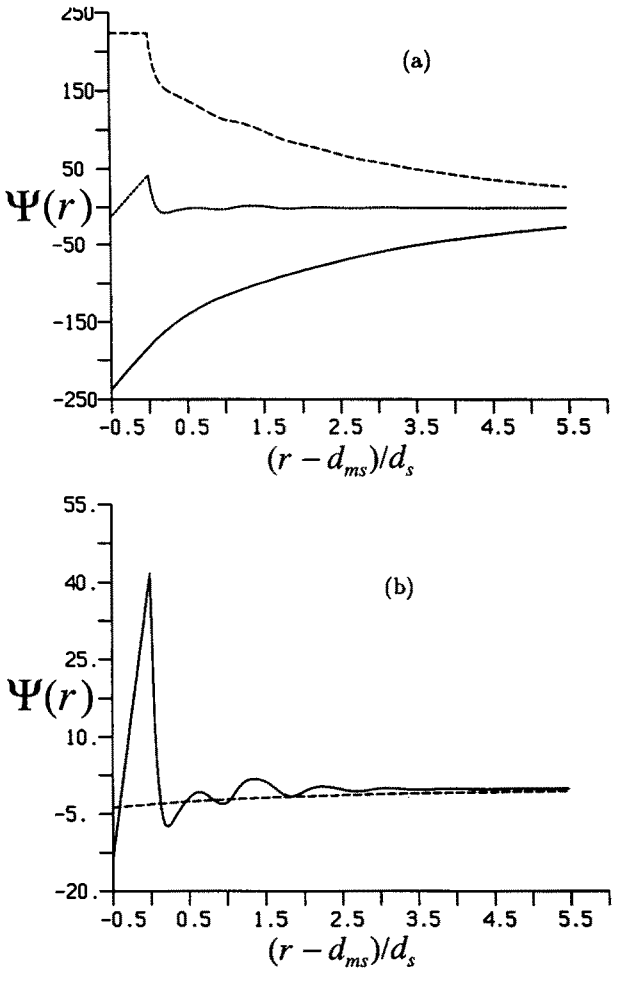

FIG. 15. (a) Contributions to the mean electrostatic potential arising from all charged species (—) and from the solvent (– –) together with the resulting total $\Psi(r)$ (···) for a macroion with $d_m = 30d_s$, $\sigma = -56$ in 0.1 M KCl. (b) Total $\Psi(r)$ for the same system as Fig. 15(a). (—) RHNC for the molecular solvent model; (– –) modified Gouy–Chapman theory for a flat surface in the corresponding continuum solvent. (Note: in all figures Ψ is expressed in units of kT/e.)

the solvent counterpart to the fast ionic screening described in Sec. III A.) We have commented before[3,4] on the resulting idiosyncratic behavior of the total potential (dotted line) which, although negative like σ *on* the surface, is very large and positive at the point of contact of a positive counterion. Even if this bizarre positive spike in $\Psi(r)$ should prove to be a consequence of the oversimplified model of the surface, it is worth noting that this is the model underlying most microscopic pictures of the double layer. In spite of this peak in $\Psi(r)$, the counterion density for this system has the customary maximum at contact [cf. the attractive well in Φ_{m+} in Fig. 1(c)]. This decoupling of the ionic distributions from the mean electrostatic potential in the region of pronounced solvent structural effects is likely a more general property of molecular solvent models. If so, that would be one important way in which such models differ qualitatively from the traditional continuum solvent picture.

In Fig. 15(b) we have redrawn the total mean electrostatic potential of Fig. 15(a) together with the modified Gouy–Chapman (MGC) potential for a planar surface with the same surface charge in a continuum solvent with the same dielectric constant as our pure molecular solvent. (We use the term modified Gouy–Chapman theory here in the manner of recent theoretical work on the primitive model double layer, to denote simply the incorporation into the classical Gouy–Chapman theory of a distance of closest approach of the ions to the surface.[10]) On the scale used in this figure the oscillatory structure in $\Psi(r)$ is more evident and of course it extends the same four diameters or so from the surface as the solvent-induced short-range structure in Φ_{m+} [cf. Fig. 4(a)]. For this 0.1 M system we were able to confirm the existence of asymptotes in the RHNC results for Φ_{m+} characteristic of a continuum solvent [cf. Eq. (4)]. This implies a similar behavior for the potential but no such asymptote could be reliably measured in $\Psi(r)$ owing to the loss of numerical accuracy in the cancellation between the ionic and solvent terms in Eq. (9). The difference in magnitude between the RHNC and MGC tails in $\Psi(r)$ at intermediate distances in this figure may not be significant for the same reason (the difference in functional forms in the expected asymptotes for the planar and spherical geometries is not significant over the range plotted here). However, any continuum-like asymptote in the RHNC potential would likely have a much lower amplitude than in the classical theory since the fast screening greatly reduces the effective macroionic charge and the potentials in Fig. 15(b) are certainly consistent with this. In fact, in the extreme case where the fast screening seems to impose a limit on the effective surface charge causing the ion response far from the surface to become independent of the actual surface charge, then the long-range part of $\Psi(r)$ presumably also becomes independent of σ. To explore these matters properly would require higher quality data for $\Psi(r)$ obtained at lower concentrations than those considered here. Whatever the exact asymptotic behavior of $\Psi(r)$, its evident domination by the short-range structural effects close to the surface is in qualitative agreement with experimental results on double layers which generally do not show clearly identifiable diffuse layer contributions except at concentrations lower than those we have used in our calculations.

In any case, the precise nature of $\Psi(r)$ at large r is a delicate question compared to the relationship of the RHNC and MGC potentials on and near the surface. Even putting aside the enormous positive peak in the molecular solvent $\Psi(r)$ at contact, the amplitudes of the remaining oscillations exceed the entire variation of the monotonic MGC potential in the figure and the surface potential in the molecular solvent is nearly four times the MGC value, -13.45 vs -3.74. (All numerical values for Ψ are expressed in units of kT/e; at room temperature $\Psi = 1$ corresponds to about 25.7 mV.) This large increase in the magnitude of $\Psi(r)$ over the primitive model value arises from the short-range structure in the molecular solvent. Since this structure is not strongly dependent on concentration $\Psi(r)$ has a much weaker dependence on concentration in relative terms than in the primitive model. For example, in Fig. 16 we show $\Psi(r)$ for the same macroion as in Fig. 15(a), $d_m = 30d_s$, $\sigma = -56$, for 0.1, 0.5, and 1.0 M KCl. The solid line in this figure is the comparable quantity in the pure solvent, $\Psi(r) - Q/(\epsilon r)$.

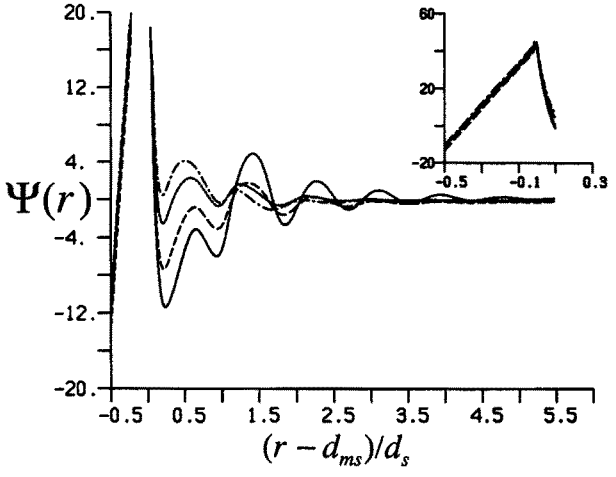

FIG. 16. $\Psi(r)$ for a macroion with $d_m = 30d_s$ and $\sigma = -56$ in various concentrations of KCl. (—) *excess* $\Psi(r)$ (see the text) in the pure solvent; (– –) 0.1 M; (···) 0.5 M; (–·–·) 1.0 M.

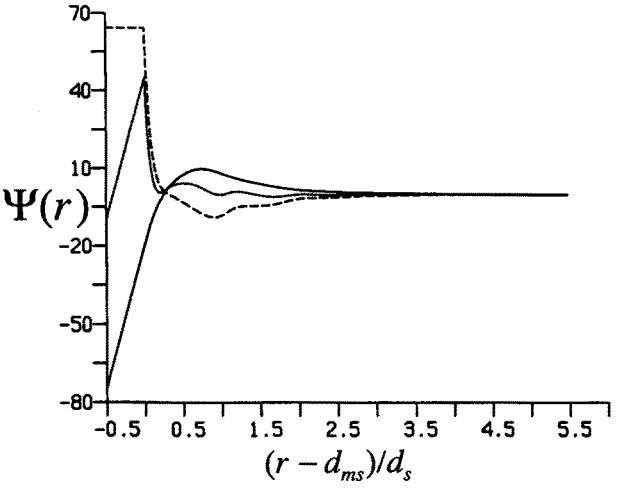

FIG. 17. Contributions to the mean electrostatic potential arising from all charged species (—) and from the solvent (– –) and the resulting total $\Psi(r)$ (···) for a macroion with $d_m = 30d_s$, $\sigma = -56$ in 1.0 M KCl.

[Strictly speaking, the most appropriate comparison would use the corresponding excess potential at finite concentration, $\Psi(r) - Be^{-\kappa r}/r$. Even had we been able to measure B reliably, however, it is clear from Fig. 15(b) that this asymptotic component of $\Psi(r)$ is so small for the concentrations we have considered that its removal would have little effect on the comparison being made in Fig. 16.] There is a spread of $3kT$ in the contact values of the potentials in this figure which is larger than the corresponding range of values in the primitive model, but which is not resolved on the scale needed here to display the molecular solvent $\Psi(r)$. The concentration dependence of the positive spike in the potential at the solvent contact distance is also not large enough to be visible on this scale. This is because a major contribution to this peak comes from the high polarization of the contact layer of solvent which is largely unaffected by concentration.

Beyond this region there is a smooth progression with concentration in the shape of the potential profiles which is characterized by a gradual dissipation in the structure in $\Psi(r)$ as the ionic screening increases. A stronger concentration dependence in $\Psi(r)$ might have been expected on the basis of the qualitative change in this screening at high concentrations, notably at 1.0 M where there is an excess neutralization of the surface charge (cf. Fig. 5). Actually, the separate solvent and ionic contributions to $\Psi(r)$ at 1.0 M, shown in Fig. 17, are quite different in shape as well as magnitude from those in Fig. 15(a) for the same macroion at 0.1 M. Nevertheless, they still combine to give a remarkably similar total potential. The near cancellation of the Coulombic and solvent polarization fields in a medium of high dielectric constant is a commonplace phenomenon of continuum electrostatics associated with the long-range behavior of the correlations in a molecular model. These results suggest that in a molecular model a similar solvent response to the free charges can operate on the scale of the short-range structure in the system. Certainly, when an oscillation in the charge density like the one implied by Fig. 5 occurs in a continuum solvent it is ordinarily accompanied by an oscillation in the potential as well.[10] Here, on the other hand, the potential at 1.0 M in Fig. 17 shows less structure, if anything, than $\Psi(r)$ at 0.1 M where $f_Q(r)$ is a monotonic function.

In theoretical work on the primitive model double layer it is customary to discuss the dependence of the surface potential on the charge density, the "equation of state" of the double layer. This is a dubious undertaking for the molecular solvent model in view of the extreme variation in $\Psi(r)$ close to the surface. For example, $\Psi(d_{m+})$ the potential at the counterion contact distance—which corresponds to what is ordinarily meant by the diffuse layer potential—has the "wrong" sign and *increases* as σ becomes more negative. Thus, both the integral and differential capacitance associated with this "diffuse layer" would, in fact, be negative. The quantity of thermodynamic significance, however, is the total potential drop Ψ_s which does have the same sign as σ and, in all systems that we have examined, satisfies the thermodynamic stability condition $d\Psi_s/d\sigma \geqslant 0$. The RHNC results for $\Psi_s(\sigma)$ are shown in Fig. 18 as points together with curves showing the corresponding MGC potential–charge relationships. (These latter are not exact for the continuum solvent case, of course, but the error is of no importance on the scale used in this figure.[10]) The molecular solvent potentials are clearly much larger than the values for a continuum solvent and are more in keeping with typical experimental values.[8] The RHNC data are obviously too sparse to allow precise estimates of the differential capacitance C_D and the wholly numerical nature of the theory precludes analysis of its functional form.[12,13] Still, for $|\sigma| \leqslant 28$ $\Psi_s(\sigma)$ is not strongly curved and we take the integral capacitance $\sigma/\Psi_s(\sigma)$ at $\sigma = -28$ as a rough estimate of $d\sigma/d\Psi_s$ at $\sigma = 0$ [an upper bound, in fact, since $\Psi_s(\sigma)$ has negative curvature]. In Table I we compare these crude estimates of C_D at the pzc with experimental data for KCl at a mercury electrode. Also included in the table are the predictions of Gouy–Chapman theory for C_D both with (MGC) and without (GC) the addition of a distance of closest approach for counterions. The very close quantitative agreement of the RHNC values

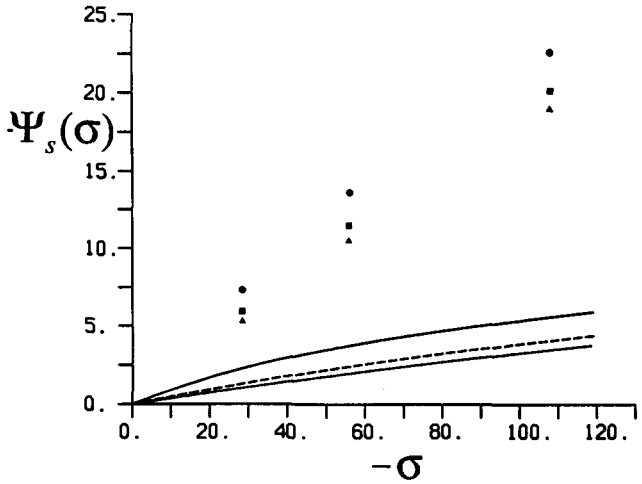

FIG. 18. Total potential drop across the double layer $\Psi_s(\sigma)$ as a function of the surface charge σ for a macroion of diameter $30d_s$ in various concentrations of KCl. The points are the RHNC results for the molecular solvent, (●) 0.1 M; (■) 0.5 M; (▲) 1.0 M. The continuous curves are the modified Gouy–Chapman predictions for a flat surface in the corresponding continuum solvent.

with the experimental numbers here is accidental, of course. The principal point of the table and Fig. 18 is, rather, that in molecular solvent models the potentials are much larger and hence the differential capacitances are much smaller than in MGC theory, especially at high concentrations. This is in qualitative accord with experimental results in real systems and can be achieved for a molecular Hamiltonian model with no adjustable parameters or specific interactions.

IV. CONCLUSION

In this paper and its two predecessors[3,4] we have described a first attempt to apply a modern liquid state theory to a model of the electrical double layer in which the solvent is treated as a molecular species with water-like parameters. This is largely uncharted territory save for earlier analyses of the limiting behavior of the mean spherical approximation (MSA) for the dipolar hard sphere solvent near the pzc;[12,13] nor has there been much reliable simulation work for water-like models at charged surfaces. Nevertheless, the RHNC theory has proved accurate in a similar context[15] and its nonlinear closure allows for coupling between orientational and radial correlations over the entire range of surface charges that characterize double layer systems. By solving the full RHNC theory for isolated macroions in solution we have obtained detailed and comprehensive information on the structure at the molecular level for the interfacial region

TABLE I. Theoretical and experimental results for the differential capacitance (F m^{-2}) of KCl at the potential of zero charge. The experimental results are those of Worsina as cited by Parsons (Ref. 14).

Conc.(M)	GC	MGC	RHNC	Expt.
0.1	0.79	0.69	0.25	0.28
0.5	1.78	1.33	0.30	...
1.0	2.49	1.71	0.34	0.39

over a wide range of surface charge densities and salt concentrations. Many aspects of this structure do not conform with conventional hypotheses regarding the short-range structure of the double layer. For example, we find almost no probability that a solvent molecule in direct contact with a highly charged surface will be aligned with its dipole parallel to the electric field of the surface. Nevertheless, this observation forms part of a coherent and consistent picture of the interface that can be understood in broad terms on the basis of two simple observations.

(1) *Intermolecular forces involving water molecules are strong and highly directional.* It is this aspect of our model that is responsible for a short-range orientational order, even at a neutral surface, that is very different from that predicted by similar theories applied to simpler models such as purely dipolar hard spheres.[16,17] This also accounts for : (1) the great sensitivity of the solvent structure to the degree of curvature of the surface; (2) the remarkable stability of an ice-like solvent arrangement for flatter surfaces that is little perturbed by either surface charge or salt concentration; and (3) short-range structure in the ion response to the charged surface that is very sensitive to ion size but not to surface charge or salt concentration. In other words, the structure of the interfacial region is the solvent's "solution" to the "problem" of minimizing the interaction energy between water molecules (by maximizing the number of tetrahedral contacts or hydrogen bonds) despite the intrusion of the surface. The resulting solvent structure then controls the short-range component of the response of ions to the surface (except for ions very close to the surface) so that this too is insensitive to surface charge and salt concentration. For both solvent and ions the influence of surface charge on all this is of secondary importance, being largely limited to the superposition onto the short-range structure of the much smaller asymptotic (continuum) behavior of the ionic density and solvent polarization profiles.

(2) *Solvent molecules and ions closer than one diameter from contact with the surface cannot be screened from the bare field of the surface charge.* For the solvent this means a very high degree of polarization for the contact layer though still in a manner compatible with the overall orientational order in the solvent at a neutral surface. This leads to the counterintuitive peak in the electrostatic potential of opposite sign to the surface charge. For counterions, the same lack of screening induces a very strong adsorption into this region which results in a very rapid neutralization (spatially) of high surface charges, a phenomenon that we describe as fast screening. As a consequence, both solvent and ions beyond this region respond as though experiencing an effective charge that is much lower than the actual surface charge. There is even evidence in our 0.1 M results of an upper limit to the magnitude of the effective charge that can be sustained, with any additional surface charge being completely neutralized by a compensating adsorption of counterions into this narrow region. It must be stressed that this adsorption is nothing more than the natural consequence of the direct Coulomb attraction of the surface for counterions where this is unmediated by intervening solvent or ions. In our simplified model this phenomenon would be very similar

for all counterions; in this sense it is the antithesis of the "specific adsorption" that is often invoked to account for experimental data. In the absence of such specific adsorption it is often supposed that cations are too strongly solvated ever to achieve direct contact with the surface in the way that our results indicate. These results may well be modified in treatments of the surface, although it is far from clear that such modifications of the model would act to reduce such adsorption. For the present water model, both the magnitude of the effect and its simple physical basis argue against dismissing it as an artifact solely on the basis of its novelty.

There are more generic aspects of these results that uphold the prejudices of liquid state theorists about the nature of the double layer in a molecular solvent and which were already demonstrated in the MSA work on dipolar spheres.[12,13] There are oscillatory components in the polarization density and the electrostatic potential as well as in the more direct measures of the interfacial structure. In most systems these oscillations are gradually attenuated giving way to continuum behavior about four solvent diameters from the surface. There is no support, then, for the notion of an "inner" layer of only molecular dimensions joined at a distinct boundary to an outer layer in which there are no discrete solvent effects. In fact, the attainment of continuum behavior as close as $4d_s$ to such a highly structured and stable region as seems to characterize water at a smooth surface would itself be more surprising were it not consistent with a growing body of results for molecular solvent models of electrolyte solutions.[1,15,18–20] The only systems in which we found solvent structural effects extending many diameters from the surface were highly charged macroions in pure solvent with no electrolyte. The complete disappearance of such effects as a result of the fast screening in salt concentrations of 0.1 M or more leaves unresolved the question of whether such phenomena are to be found at much lower finite concentrations. This is an interesting possibility because any such large σ effect must depend only on the coupling between the molecular dipoles and the surface field, giving it a generality that would transcend the details of particular water models.

These calculations have demonstrated the feasibility of applying a relatively sophisticated statistical mechanical theory to a wholly molecular model of the solution side of an aqueous electrical double layer. Of course, we remain far from possessing a comprehensive understanding of such systems at the molecular level. We have already mentioned at several points in the discussion the desirability of extending the present calculations to lower concentrations, particularly in order to clarify their relationship to the classical Gouy–Chapman theory. This happened to be awkward to do with the particular algorithms and computing resources used in this work but there is no fundamental obstacle to such an extension. The relationship in the RHNC theory of the double layer structure at these curved surfaces to that at a perfectly plane wall remains to be established; this is important for comparison with other theories and computer simulations using the latter geometry.

And finally, of course, there are many possible variations on the model that could be considered. Even for a mercury electrode, the observable properties of double layers show strong dependence on the specific nature of the counterion, especially for anions.[8] This is manifested, for example, in strong asymmetries about the pzc in the differential capacity which are ordinarily ascribed to specific interactions between the surface and the ions.[11] In our highly simplified model one ionic species is distinguished from another solely by its hard sphere diameter. Although this can scarcely be expected to provide the latitude necessary to account for the rich variety of behavior observed experimentally it certainly was sufficient to cause a wide range of behavior in our earlier results for the macroion–counterion potentials of mean force at infinite dilution.[4] KCl is actually an exceptional case on account of the closeness of the cation and anion sizes to each other and to that of the solvent. That is, the solvent structural effects on the ion density profiles that we have described here will be relatively small and unusually symmetric about $\sigma = 0$ compared to similar models with greater size asymmetry between cations and anions. We are currently investigating the RHNC predictions for the structure of double layers in the corresponding model of NaCl for which our earlier infinite dilution results[4] revealed very large short-range structural effects in the response of the small cation to the surface. We are also applying the theory to the surface behavior of a more refined solvent model incorporating accepted values for the quadrupole and octupole moments of the molecular charge distribution. In contrast to the charge-symmetric solvation property of the tetrahedral solvent used here, this improved model exhibits marked preferential solvation of anions in bulk solution[2] and is capable in principle, then, of producing surface structures with appreciable asymmetry about a large nonzero pzc. We are now in a position to build up a body of results for a variety of such molecular solvent models from this and alternate theoretical approaches. Once the consequences for double layer properties of simple models such as these are better understood the way will be open to a better appreciation of the role played by specific interactions in such systems.

ACKNOWLEDGMENTS

This work has been supported in part by the Defence Research Board of Canada under ARP award 3610-645, and in part by the Natural Sciences and Engineering Research Council of Canada. Acknowledgment is made to the Donors of the Petroleum Research Fund, administered by the American Chemical Society, for partial support of this research.

[1] P. G. Kusalik and G. N. Patey, J. Chem. Phys. **88**, 7715 (1988).
[2] P. G. Kusalik and G. N. Patey, J. Chem. Phys. **89**, 5843 (1988).
[3] G. M. Torrie, P. G. Kusalik, and G. N. Patey, J. Chem. Phys. **88**, 7826 (1988).
[4] G. M. Torrie, P. G. Kusalik, and G. N. Patey, J. Chem. Phys. **89**, 3285 (1988).
[5] C. Y. Lee, A. J. McCammon, and P. J. Rossky, J. Chem. Phys. **80**, 4448 (1984).
[6] G. N. Patey, J. Chem. Phys. **72**, 5763 (1980).
[7] G. M. Torrie and J. P. Valleau, J. Chem. Phys. **81**, 6291 (1984).

[8]D. C. Grahame, Chem. Rev. **41**, 441 (1947).
[9]J. O'M. Bockris and A. K. Reddy, *Modern Electrochemistry* (Plenum, New York, 1970), Vol. 2.
[10]S. L. Carnie and G. M. Torrie, Adv. Chem. Phys. **56**, 141 (1984).
[11]M. A. Habib and J. O'M. Bockris, in *Comprehensive Treatise of Electrochemistry*, edited by J. O'M. Bockris, B. E. Conway and E. Yeager (Plenum, New York, 1980), Vol. 1.
[12]S. L. Carnie and D. Y. C. Chan, J. Chem. Phys. **73**, 2949 (1980).
[13]D. Henderson, L. Blum, and M. Lozada-Cassou, J. Electroanal. Chem. **150**, 291 (1983).
[14]R. Parsons, *Modern Aspects of Electrochemistry*, edited by J. O'M. Bockris and B. E. Conway (Butterworth, London, 1954), Vol. 1.
[15]J. M. Caillol, D. Levesque, J. J. Weis, P. G. Kusalik, and G. N. Patey, Mol. Phys. **62**, 461 (1987).
[16]W. Dong, M. L. Rosinberg, A. Perera, and G. N. Patey, J. Chem. Phys. **89**, 4994 (1988).
[17]D. Levesque and J. J. Weis, J. Stat. Phys. **40**, 29 (1985).
[18]G. N. Patey and J. P. Valleau, J. Chem. Phys. **63**, 2334 (1975).
[19]S. A. Adelman and J. H. Chen, J. Chem. Phys. **70**, 4291 (1979).
[20]B. M. Pettit and P. J. Rossky, J. Chem. Phys. **84**, 5836 (1986).

The Journal of Chemical Physics is copyrighted by the American Institute of Physics (AIP). Redistribution of journal material is subject to the AIP online journal license and/or AIP copyright. For more information, see http://ojps.aip.org/jcpo/jcpcr/jsp
Copyright of Journal of Chemical Physics is the property of American Institute of Physics and its content may not be copied or emailed to multiple sites or posted to a listserv without the copyright holder's express written permission. However, users may print, download, or email articles for individual use.